https://doi.org/10.62753/ctp.2003.24.7.7

Yuanding Huang[1], Norbert Hort[2], Karl Ulrich Kainer[3]
GKSS Research Center, Institute for Materials Research, Center for Magnesium Technology, Max-Planck-Strasse 1, D-21502, Geesthacht, Germany

THERMAL BEHAVIOR OF AlSi12CuMgNi PISTON ALLOY WITH AND WITHOUT SHORT FIBER REINFORCEMENT

Mismatch in thermal expansion coefficients could introduce large thermal stress and correspondingly increase the dislocation density in metal matrix composite. The aging behavior could therefore be modified. The CTE mismatch also affects the dimensional stability of metal matrix composites during their service because any fluctuation in environmental temperature could introduce internal thermal stress. The paper presents an overview on our investigations on the thermal behavior of AlSi12CuMgNi piston alloy with and without short fiber reinforcement, including aging, thermal expansion and thermal cycling behaviors. Major experimental results obtained up to now are shown and related physical phenomena are discussed.

Key words: metal matrix composite, thermal expansion, thermal cycling, piston alloy

WPŁYW TEMPERATURY NA ZACHOWANIE SIĘ CZYSTEGO I ZBROJONEGO KRÓTKIMI WŁÓKNAMI STOPU AlSi12CuMgNi PRZEZNACZONEGO NA TŁOKI SILNIKOWE

Niedopasowanie współczynników rozszerzalności termicznej (CTE) może powodować duże naprężenia termiczne i w rezultacie zwiększyć gęstość dyslokacji w kompozycie o osnowie metalowej. Dlatego jego zachowanie może zmieniać się przy starzeniu. Niedopasowanie CTE wpływa także na stabilność wymiarową kompozytów metalowych w trakcie ich użytkowania, ponieważ każda zmiana temperatury otoczenia może wywołać wewnętrzne naprężenia termiczne. Niniejszy artykuł przedstawia przegląd badań nad zachowaniem się niezbrojonego i zbrojonego krótkimi włóknami stopu przeznaczonego na tłoki silnikowe pod wpływem temperatury przy starzeniu, rozszerzaniu cieplnym i pod działaniem cyklicznego obciążenia termicznego. Przedstawiono najważniejsze wyniki dotychczasowych badań i omówiono związane z tym zjawiska fizyczne.

Słowa kluczowe: kompozyt o osnowie metalowej, rozszerzalność cieplna, cykliczne obciążenie termiczne, stop na tłoki silnikowe

INTRODUCTION

The dislocation density is generally increased in the interface region in metal matrix composites (MMCs) and the chemical composition could be modified as a consequence of segregation. All these aspects may change the kinetics of precipitation and the interfacial reaction. These changes will further affect the mechanical properties and performance of MMCs. The investigations on aging behavior of Al-Si alloy based composites have shown that the aging is often accelerated as compared with the unreinforced alloys [1].

Any fluctuation in environmental temperature will introduce internal thermal stress due to the large difference on the coefficients of thermal expansion (CTE) between the matrix and ceramic reinforcement [2]. This residual stress has a substantial effect on the dimensional stability and damage-tolerant properties, and also strongly affects the thermal expansion [3]. Strain hysteresis loop is often observed between the heating and cooling cycles [4, 5]. It has been shown that thermal cycling represents a more severe condition than equivalent time at the high temperature of thermal cycling [5].

The investigation of thermal cycling behavior has received less attention for the reinforced AlSi12CuMgNi (KS1275®) piston alloy, especially the effect of reinforcement and heat treatment. This paper presents an overview on our investigations on its thermal behavior, including aging, thermal expansion and thermal cycling behaviors. Major experimental results obtained up to now are shown and related physical phenomena are discussed.

EXPERIMENTAL PROCEDURES

Four composites were selected to investigate their thermal behavior: AlSi12CuMgNi (KS1275®)+20% Saffil® (> 95% δ-Al_2O_3, < 5% SiO_2), KS1275®+20% Maftech® (~72% δ-Al_2O_3, ~28% SiO_2), KS1275®+20% Kaowool® (~47% δ-Al_2O_3, ~53% SiO_2) and KS1275®+ +20% Supertech® (~65% SiO_2, ~31%CaO, 4% MgO). The aluminum alloy matrix (KS 1275®) selected has a composition (wt.%) of 11~13.5 Si, 0.5~1.3 Cu,

[1] Ph.D., [2] Dr.-Ing., [3] Prof. Dr.-Ing.

0.8~1.3 Mg, 0.5~1.3 Ni, ~0.25 Zn, ~0.1 Cr, balance Al. The reinforced composites were fabricated by direct squeeze casting technique. In the process, the preform supplied by Thermal Ceramics de France with a size of 100 mm (diameter) × 20 mm (thickness) was held in a die heated at 200°C. Among the preforms used, both the Saffil® and Maftech® fibers exhibit a crystal structure, and both the Kaowool® and Supertech® fibers exhibit an amorphous structure since the X-ray diffraction patterns show no peaks for these two fibers. These preforms contained 20% reinforcement predominately and randomly oriented in the plane of the disc. Molten aluminum alloy was then poured into the die with an applied pressure of 8 MPa.

The microstructures of composites were observed on both the longitudinal and transverse sections using optical microscopy in as-polished condition. The aging behavior of both the unreinforced alloy and composites were investigated by Vickers hardness tests. For the composites, the microhardness was investigated on their transverse sections. All samples were first solution treated at 510°C for 8 hours and then they were age treated at 200°C for various time followed by air cooling. Hardness tests were carried out using a HMV 2000 machine with a load of 19.6 N and a holding time of 10 s. Ten points have been evaluated for each specimen.

The X-ray investigations were carried out to identify phases in the materials using a Siemens diffractometer operating at 40 kV and 40 mA with CuK_α radiation. Measurements were performed by step scanning 2θ from 15 to 120° with a step size of 0.03°. A count time of 3 s per step was used. Slow scan in a defined 2θ range was also conducted using a step size of 0.01° and a count time of 15 s per step in order to increase the resolution and to try to detect the phases with small amount. The X-ray diffraction has shown to be an effective method to identify the phases in the AlSi12CuMgNi alloy [6].

The investigations of both the CTE and thermal cycling were performed using a quartz tube dilatometer Netzsch Thermische Analyse DIL 402C equipped with TASC 414/3 controller. The longitudinal and transverse specimens used for both the CTE measurement and thermal cycling were rectangular with a length of 10 mm and a cross-section area of 5x5 mm. Both the unreinforced and reinforced samples were cycled 47 times over a temperature range from 58 ±2 to 287 ±5°C. Each cycle consists of heating and cooling with a rate of 10°C/min. The technical expansion coefficient for the temperature interval $T_2 - T_1$ that is defined as

$$\alpha(T_2 - T_1) = \frac{\frac{\Delta L}{L_0}(T_2) - \frac{\Delta L}{L_0}(T_1)}{T_2 - T_1} \quad (1)$$

and was calculated from both the first (heating) and second (cooling) segments of thermal cycling curve. Where T_1 is the lower temperature limit (90°C was chosen in the present work), T_2 is the upper temperature limit (270°C was chosen in the present work), L_0 is the sample length measured at ambient temperature and ΔL is the increment of sample length when the temperature is increased to T_1 or T_2. The microhardness on the transverse section was measured after thermal cycling to evaluate the possible change of mechanical properties. The parameters for the hardness test were the same as those mentioned above.

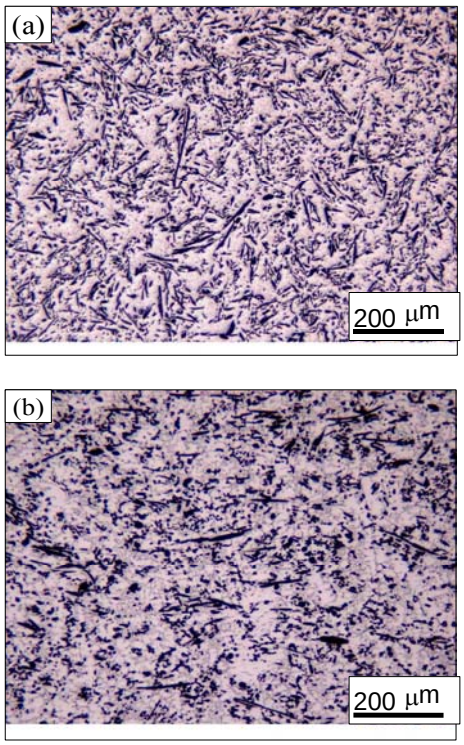

Fig. 1. Microstructure of as-cast materials: a) KS1275®+Saffil®, longitudinal section; b) KS1275®+Saffil®, transverse section

EXPERIMENTAL RESULTS AND DISCUSSION

Optical microstructure

Figure 1 shows a typical optical microstructure for the as-cast Saffil® fiber reinforced KS1275® alloy. It is shown that the fibers remain predominantly in a planar-random arrangement with relatively few parallel to the disc axis after the infiltration process. The aspect ratio of the short fiber was measured to be about 4.5. There is no large difference in microstructure among the composites. Whereas the unreinforced alloy shows a pronounced dendritic structure, this is not the case in the composites because the free dendritic growth is restricted by the reinforcements. The matrix grains in

the composites are smaller than those of the unreinforced alloys.

Aging behavior

Figure 2 shows the microhardness as a function of annealing time for the alloys annealed at 200°C. The addition of reinforcement increases the microhardness except for the Kaowool® fiber. The composites containing the Saffil® and Maftech® fibers have a higher microhardness. The difference in hardness of composites could be related to the different strengthening effects of reinforcements. It was reported that the tensile strength is about 2000 and 1300 MPa for the Saffil® and Kaowool® fibers, respectively [4]. The hardness begins to increase after an incubation time for the unreinforced alloy. The composites containing the Saffil® and Maftech® fibers show an increase in the hardness without any incubation time. With increasing in annealing time, the hardness first increases and reaches a maximum, and then decreases and tends to be constant. However, it keeps almost unchanged for the Kaowool®-reinforced alloy in the whole range of aging time. Compared with the unreinforced alloy, the appearance of the aging peak is shifted to an earlier time for the alloys reinforced with the Saffil®, Maftech® and Supertech® fibers.

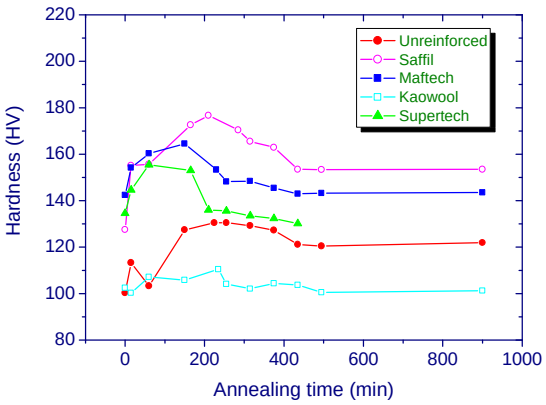

Fig. 2. Microhardness as a function of annealing time for both the unreinforced and reinforced alloys annealed at 200°C after they were performed solution heat treatment at 510°C for 8 hours

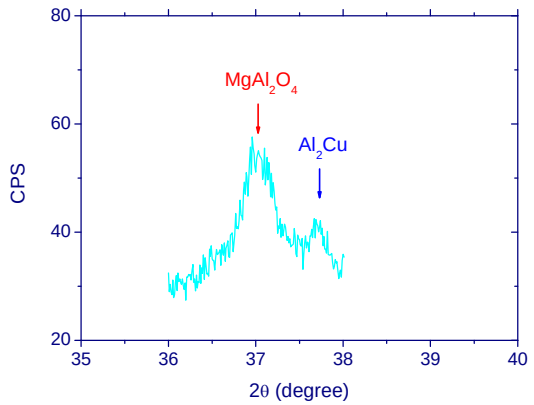

Fig. 3. X-ray diffraction pattern showing the peaks for the $MgAl_2O_4$ and Al_2Cu phases in the as-cast Kaowool®-reinforced alloy. The slow scan with a step size of 0.01° and a count time of 15 s per step was used

Table 1 lists the phases in both the as-cast and peak aging-treated alloys identified by X-ray diffraction. Besides the aluminum, silicon and reinforcements, the X-ray experiments detected the phases Al_2Cu and Mg_2Si in each as-cast material. The Al_2Cu phase was also detected in each aging-treated alloy, but the Mg_2Si phase cannot be detected in the aging-treated composite containing the Kaowool® fiber. The AlCuMg phase was detected in both the KS1275® alloy and KS1275®+ +Saffil® alloy with and without aging treatment, but could not be detected in the other alloys. The peaks of the spinel phase $MgAl_2O_4$ were observed in both the as-cast and aging-treated composites except for the Saffil®-reinforced composite (Fig. 3). It was reported that the phases Mg_2Si, AlCuMg, Al_3Ni, Al_2Cu and $MgAl_2O_4$ have been detected in both the as-cast and aged AlSi12CuMgNi alloy reinforced with the Saffil® fiber using X-ray diffraction method [6].

TABLE 1. **Phase analysis in both the as-cast and aging-treated alloys. The matrix (Al and Si) and reinforced phases are not listed**

Alloy	KS1275®	+Saffil®	+Maftech®	+Kaowool®	+Supertech®
As cast	Al_2Cu Mg_2Si AlCuMg	Al_2Cu Mg_2Si AlCuMg	Al_2Cu Mg_2Si $MgAl_2O_4$	Al_2Cu Mg_2Si $MgAl_2O_4$	Al_2Cu Mg_2Si $MgAl_2O_4$
After peak aging	Al_2Cu Mg_2Si AlCuMg	Al_2Cu Mg_2Si AlCuMg	Al_2Cu Mg_2Si $MgAl_2O_4$	Al_2Cu $MgAl_2O_4$	Al_2Cu Mg_2Si $MgAl_2O_4$

The accelerated aging is a well known effect in MMCs with age-hardenable matrix alloys [1, 7, 8]. The dislocation density is increased near the reinforcement due to the introduction of thermal stress arising from the CTE mismatch between the matrix and reinforcement. The increase in dislocation density can cause an increase of the diffusivity of solute atoms and accelerate the solute segregation and the precipitation near the interface. The phase analysis indicates that the precipitations are related to the content of SiO_2 in the alloys which comes from the binder or the reinforcement. The spinel $MgAl_2O_4$ is produced due to the reaction of SiO_2 with magnesium [9], leading to the depletion of strengthening phase Mg_2Si and AlCuMg and the weakening of age hardening (see Fig. 2). The hardening even disappears in the Kaowool®-fiber reinforced alloy in which the content of SiO_2 is high.

Thermal expansion

Figure 4 shows the evolution of CTE during thermal cycling to 47 cycles. The CTE was calculated from each cycle according to the equation (1) with the temperature range from 90 to 270°C. First, the CTE of longitudinal samples has been checked (Fig. 4a). The CTEs of all composites are lower than that of the unreinforced alloy, indicating that the additions of Saffil® or Maftech® fibers are effective in decreasing the CTE of AlSi12CuMgNi alloy. The decrease in CTE is due to the fact that the matrix of these samples has a higher mechanical constraint from the reinforcement. For both the unreinforced and Maftech®-fiber reinforced alloys, their CTEs are stable during the whole thermal cycling. However, the CTE of Saffil®-reinforced alloy largely changes at the early stage of thermal cycling and tends to be stable at the later stage. The different evolution of CTE could be related to the different [illegible]. In the Maftech®-fiber reinforced [illegible] of interfacial reaction that is caused [illegible] magnesium with the SiO_2 ma[illegible] improv[illegible]ding. The improvement of interfaci[illegible] from the interfacial reaction was also reported by Baxter [10].

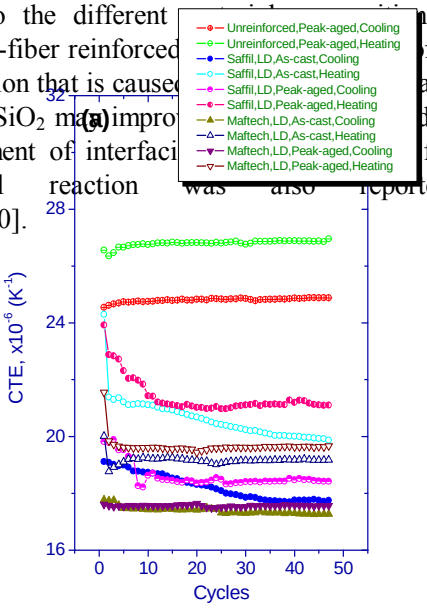

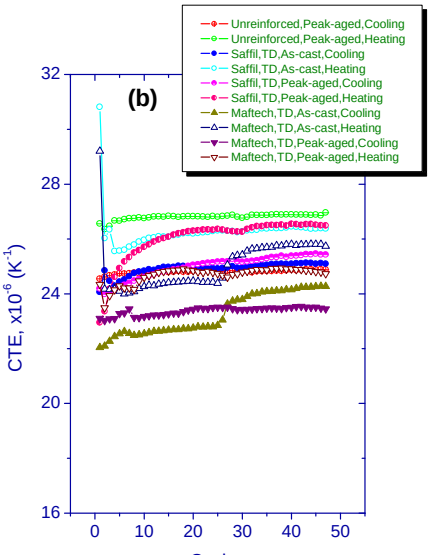

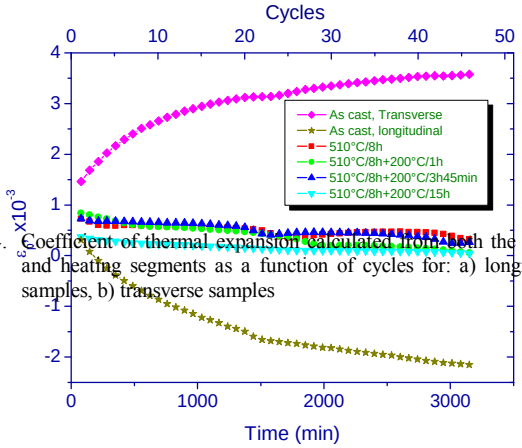

Fig. 4. Coefficient of thermal expansion calculated from both the cooling and heating segments as a function of cycles for: a) longitudinal samples, b) transverse samples

Fig. 5. Residual strain after thermal cycling as a function of both thermal cycling time and cycles for the unreinforced KS1275 alloy ε_p is the residual strain

Compared with the CTEs of longitudinal samples, the CTEs of transverse samples are larger (Fig. 4b). In addition, the CTE is not so stable as that observed for the longitudinal samples. For the transverse sample, the constraint from the reinforcement on the matrix is small. The matrix is easy to deform elastically or plastically along this direction.

As shown in Figure 4, a larger CTE was calculated from the first heat segment for the as-cast materials. Further thermal cycling leads to a sharp decrease in CTE. No such phenomenon was observed in the peak-aged materials. This difference may be caused by the different internal stress state inside the materials. Normally, the internal stress is complicated and large inside the as-cast materials, which have been generated by the squeezing pressure and by the subsequent solidification. For the aging-treated alloy, the previous thermal stress generated during squeeze casting may have been released and new thermal stress could be produced during the subsequent cooling. This thermal stress should be smaller than that generated during squeeze casting.

Finally, the CTE calculated from the heating segment is different from that calculated from the cooling segment. The former is much larger than the latter. During the heating stage, the internal stress generated during squeeze casting could be released and correspondingly the squeeze cast materials begin to loosen. The sample length increases rapidly once the sample starts to relax.

To some degree, this can also explain why a larger CTE has been measured from the first heating segment for the as-cast samples.

Thermal cycling

Figure 5 shows the residual strain after each thermal cycling as a function of both the time and thermal cycles for the unreinforced alloy. The definition of residual strain ε_p is referred to Ref. [11]. It is shown that the residual strain of as-cast sample changes largely during thermal cycling, but that of the heat treated samples changes a little, even for the solution treated sample followed by water quenching. For this sample, it has a very high cooling rate that is possible to induce large thermal stresses. However, its residual strain change is similar to that of the samples with aging treatment (in these samples, the thermal stress is low because the aging temperature is only 200°C). The thermal stress generated during cooling plays a negligible role in affecting the residual strain. For the as-cast unreinforced alloy, it has a larger thermal stress arising not only from the squeeze pressure but also from the thermal stress. The phenomenon decided above indicates that the internal stress arising from the squeeze casting, especially the squeeze pressure, largely affects the residual strain induced in the subsequent thermal cycling.

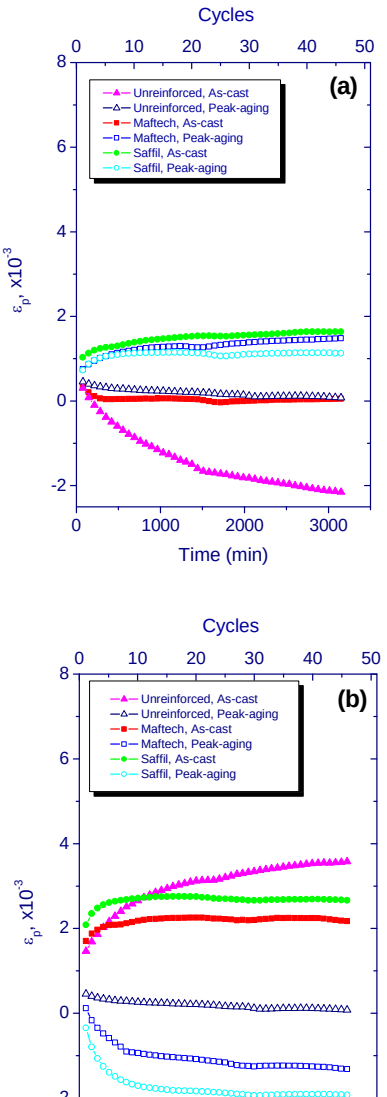

Fig. 6. Residual strain after thermal cycling as a function of both time and cycles: a) longitudinal samples; b) transverse samples. The peak aging process was carried out based on the results mentioned in the section of „aging behavior"

Figure 6 shows the residual strain after thermal cycling as a function of both time and cycles for the unreinforced and reinforced alloys with and without peak-aging treatment. For the longitudinal specimens, the residual strain of the unreinforced alloy has a larger change during the thermal cycling, but it is more stable for the composites. For the transverse specimens, the situation is different: the residual strain changes largely not only for the unreinforced alloy but also for the composites. In the composites, more change in residual strain is mainly at the early stage of thermal cycling. As shown in Figure 6, the peak-aging treatment also affects the thermal residual strain in composites. Firstly, the residual strain is different between the as-cast and peak-aged specimens at the same cycles. Secondly, trend of the changing in residual strain is different before and after aging treatment. After peak aging, the residual strain of the longitudinal specimen increases with the thermal cycling proceeding, but decreases for the transverse specimens. Finally, unlike the unreinforced alloys, the change in residual strain is almost same in the composites before and after heat treatment. These phenomena could be related to the change of internal stress after the peak-aging treatment was performed (see above discussion).

TABLE 2. **Microhardness of as-cast materials before and after thermal cycling**

Materials	Microhardness (HV)		
	As cast	After 15 cycles	After 47 cycles
Unreinforced	98.3[a] ±3.7[b]	NA[c]	77.0 ±1.3
+Saffil®	139.3 ±6.3	118.9 ±2.3	108.4 ±3.0
+Maftech®	132.4 ±5.8	117.4 ±7.6	101.9 ±7.4
+Kaowool®	131.2 ±5.6	98.9 ±4.4	NA
+Supertech®	122.0 ±4.4	96.1 ±4.5	NA

[a] average value, [b] standard deviation, [c] not available

Table 2 lists the microhardness of both the as-cast unreinforced and reinforced alloys before and after thermal cycling. Cycling of unreinforced alloy and composites results in a decrease of hardness. After calculating the hardness difference before and after 47 thermal cycles, it is known that the hardness difference for the unre-

inforced alloy is not much lower than that for the Saffil®- and Maftech®-reinforced alloys. It is 21.3, 30.9 and 30.5 for the unreinforced alloy, the Saffil®-reinforced alloy and the Maftech®-reinforced alloy, respectively. For the unreinforced alloy, the reduction in hardness should be related to the relaxation of previous thermal stress or overaging. The more reduction in hardness in composites could be explained as follows: firstly, the aging is accelerated in the composites due to the increase of dislocation density, it could be expected that the overaging is much heavier in the composites than that in the unreinforced alloy. Secondly, more thermal stress has been released in the composite because the composite has a higher initial thermal stress caused by a high dislocation density. Therefore, it is reasonable to conclude that the more reduction in microhardness is caused by much heavier overaging and matrix recovery rather than by the interface debonding.

CONCLUSIONS

The aging in composites is accelerated due to the introduction of high density dislocation. The precipitation is related to the composition of alloys investigated. The spinel phase $MgAl_2O_4$ is formed due to the reaction of SiO_2 with magnesium. The thermal stress generated during squeeze casting affects both the thermal expansion and thermal cycling behaviors. The thermal stress generated from the squeeze pressure plays an important role in producing residual strain after thermal cycling. Both the thermal expansion and thermal cycling behaviors are also affected by the subsequent heat treatments. The thermal cycling results in a decrease in micro- hardness that is due to the overaging and matrix recovery.

Acknowledgements

The authors wish to thank Mr. Hajo Dieringa and Mrs. Joanna Dzwonczyk for helpful discussions and Mr. Volker Kree for technical assistance. Financial supported by Deutsche Forschungsgemeinschaft (DFG) under Project number K171053/4-1 is also gratefully acknowledged.

REFERENCES

[1] Bär J., Gudladt H.J., Illy J., Lendvai J., Influence of fiber reinforcement on the aging behavior of an AlSi12CuMgNi alloy, Mater. Sci. Eng. 1998, A248, 181-186.

[2] Kiehn J., Smola B., Vostry P., Stulíková, Microstructure changes in isochronally annealed alumina fiber reinforced Mg-Ag-Nd-Zr alloy, Phys. Stat. Sol. 1997, 164, 709-723.

[3] Neite G., Mielke S., Thermal expansion and dimensional stability of aluminum fiber reinforced aluminum alloys, Mater Sci. Eng. 1991, A148, 85-92.

[4] Clyne T.W., Withers P.J., An introduction to metal matrix composite, Cambridge University Press, Cambridge 1993.

[5] Chmelik F., Lukàc P., Kiehn J., Mordike B.L., Kainer K.U., Langdon T.G., Characteristics of thermal cycling in a magnesium alloy composite, Mater. Sci. Eng. 2002, A325, 320-323.

[6] Akbulut H., Durman M., Yilmaz F., A comparison of as-cast and heat treated properties in short fiber reinforced Al-Si piston alloys, Scripta Materialia 1997, 36(7), 835-840.

[7] Vogelsang M., Arsenault RJ., Fisher RM. An in situ HVEM study of dislocation generation at Al/SiC interfaces in metal matrix composites, Metall. Trans. 1986, 17A(3), 379-389.

[8] Christman T., Needleman A., Nutt S., Suresh S., On microstructural evolution and micromechanical modeling of deformation of a whisker-reinforced metal matrix composite, Mater. Sci. Eng. 1989, A107, 49-61.

[9] Pai B.C., Ramani G., Pillai R.M., Satyanarayana K.G., Role of magnesium in cast-aluminum alloy matrix composites, J. Mater. Sci. 1995, 30, 1903-1911.

[10] Baxter W.J., Sachdev A.K., The tensile strength of 339 aluminum reinforced with Kaowool fibers: a comparison of T5 and T6 heat treatment, Metall. Trans. 1999, 30A, 1835-1841.

[11] Huang Y., Hort N., Kainer K.U., Thermal behavior of short fiber reinforced AlSi12CuMgNi piston alloys, Kompozyty (Composite) 2003, 3, 6.

Recenzent
Władysław Włosiński